NJC

Accepted Manuscript

This is an *Accepted Manuscript*, which has been through the Royal Society of Chemistry peer review process and has been accepted for publication.

Accepted Manuscripts are published online shortly after acceptance, before technical editing, formatting and proof reading. Using this free service, authors can make their results available to the community, in citable form, before we publish the edited article. We will replace this *Accepted Manuscript* with the edited and formatted *Advance Article* as soon as it is available.

You can find more information about *Accepted Manuscripts* in the Information for Authors.

Please note that technical editing may introduce minor changes to the text and/or graphics, which may alter content. The journal's standard Terms & Conditions and the Ethical guidelines still apply. In no event shall the Royal Society of Chemistry be held responsible for any errors or omissions in this *Accepted Manuscript* or any consequences arising from the use of any information it contains.

ROYAL SOCIETY OF CHEMISTRY

www.rsc.org/njc

Journal Name

ARTICLE

Graphene oxide-TiO_2 composites: an efficient heterogeneous catalyst for the green synthesis of pyrazoles and pyridines†

Shweta Kumari,[a] Amiya Shekhar,[b] and Devendra D. Pathak[a,*]

0Received 00th January 20xx,
Accepted 00th January 20xx

DOI: 10.1039/x0xx00000x

www.rsc.org/

Graphene oxide-TiO_2 composites (GO-TiO_2), has been synthesized and characterized by FT-IR, FT-Raman, XRD, XPS, FESEM, EDAX, TEM and N_2 adsorption-desorption. The GO-TiO_2 has been found to be highly efficient and recyclable heterogeneous catalyst for the synthesis of pyrazoles and pyridines in aqueous medium at room temperature.

Introduction

Graphene oxide (GO), has aroused considerable interest, due to owing to its high specific surface area, presence of various oxygen functionalities, structural defects, high mechanical strength and excellent electrical conductivity.[1] The oxygen functionalities which are placed in GO have been recognized as anchoring sites for chemical functionalization, inorganic complexes and nanoparticles immobilization, etc.[2] GO based materials have to found various applications in nanoelectronics, sensors, super capacitors, semiconductor devices, and photo-catalysis.[3,4] Recently GO and its composites have been reported as catalysts for many useful organic transformations.[5]

Titanium dioxide (TiO_2) has been the most famous photocatalyst under UV light.[6] However, it has also been widely used in a variety of applications such as energy conversion, pollutants degradation and water splitting due to its low cost and high chemical stabilty.[7] In recent year much interests has been devoted for developing visible light active TiO_2 by modify TiO_2 with nanostructured carbonaceous materials.[8] GO-TiO_2 composites have been used as a heterogeneous photocatalyst for the degradation of pollutants, the water photocatalytic splitting, and antibacterial application.[9] Hybridization of GO-TiO_2 composites have not been much used in organic transformation as a heterogeneous catalysts. Recently Josephine et al. have reported, GO-TiO_2 used as a heterogeneous catalyst for esterification of benzoic acid with dimethyl carbonate.[10]

Synthesis of heterocyclic compounds using green approaches has fascinated many chemists due to easy separable, environmental friendly and cost-effective nature.[11] Pyrazoles and pyridines are important class of heterocyclic compounds.[12] Pyrazole derivatives are used in medicinal chemistry since they form the nucleus of many commercially available drugs, for example Acomplia, Viagara, Celebrex and Zometapina.[13] In addition they have also been used as ligands, chiral catalysts, synthesis of dyes, florescence and luminescence.[14] However, pyridine derivatives are used in anti-bacterial, anti-prion, anti-hepatitis B virus, and anti-cancer agents.[15]

A perusal of the literature reveals that several methods reported for the synthesis of pyrazole derivatives, such as $Cu(OAC)_2$, PTSA, $(PyPyr)_2$, $Ti(NMe_2)_2$, $Sc(OTf)_3$, $Yb(PFO)_3$, and H_2SO_4 etc[16] and for the synthesis pyridine derivatives, such as $ZrOCl_2{\cdot}8H_2O/NaNH_2$ in $[bmim]BF_4$ under ultrasound irradiation, Et_3N, DBU, piperidine, KF/alumina, $K_2CO_3/KMnO_4$, $ZnCl_2$, silica nanoparticles, boric acid, nano MgO Zn(II) and Cd(II) MOFs, etc.[17] However, many of these reported synthetic protocols suffer from one or more disadvantages, such as using toxic reagents, prolong reaction time, strong acidic or basic conditions, moderate yields, use of expensive catalyst, tedious steps, and formation of by-products. The importance of pyrazoles and pyridines in medicinal chemistry has continually attracted for, novel protocol.[18]

Herein, we report the synthesis of Graphene oxide-TiO_2 composites (GO-TiO_2), and demonstrate its application as, inexpensive, reusable and efficient heterogeneous catalyst for the synthesis of pyrazoles and pyridines derivatives in aqueous medium at room temperature in high yields.

Experimental

Synthesis of GO-TiO_2 composites

GO was synthesized by the modified Hummer's method.[19] The GO-TiO_2 composites was *in situ* synthesized based on Patra et al.'s work[20] with modifications. The composites was prepared by *in situ* reaction of $Ti(OiPr)_4$ and GO sheets. In brief, 100 mg GO was added to a 10 mL of distilled water and sonicated for 15 min, and then add 1.0 g ammonium chloride and 0.8 g sodium salicylate. The solution was stirred for 30 min, then 2 mL ammonia solution was added and the mixture stirred again for 30 min. $Ti(OiPr)_4$ (5 mmol), was then taken in 2.5 g isopropyl alcohol and this solution was slowly added to the GO solution. The *p*H of the solution was then adjusted to *p*H = 10 by addition of ammonia solution and stirred for 5 h. The mixture was hydrothermally heated to at 100°C for 48 h. The resultant solids were collected by centrifuged. The resultant solid was calcined at 773 K for 6 h to obtain the desired GO-TiO_2 composites.

General procedure for the synthesis of pyrazoles derivatives

To equimolar ratios of aldehyde (1 mmol), malononitrile (1mmol), and phenyl hydrazine (1 mmol), were dissolved in water (5 mL) at room temperature, GO-TiO_2 (10 mg) was added as catalyst. Reaction mixture was continuously stirred for 10-20 min. The progress of the reaction was monitored by TLC. After completion, GO-TiO_2 catalyst removed by filtration. The GO-TiO_2 was further washed with ethanol (3x5 mL) and then dried under vacuum for reuse. Filtrate was treated with ethyl acetate (3x10 mL). The combined organic layers were treated with saturated brine solution and dried over anhydrous sodium sulphate. The removal of solvent yielded (82-98%) products. Furthermore, the synthesized pyrazoles products were analyzed by ^1H NMR and IR spectra.

Spectral data of selected pyrazoles products

5-Amino-1-phenyl-3-phenyl-1*H*-pyrazole-4-carbonitrile(4a):
Light yellow solid: ^{1}H NMR (400 MHz, $CDCl_3$) δ = 6.80 (t, 1H, ArH), 7.00 (d, 2H, ArH), 7.11 (t, 2H, ArH), 7.18 (t, 1H, ArH), 7.45 (t, 2H, ArH), 7.69 (d, 2H, ArH), 7.80 (s, 2H, NH_2); IR (KBr, cm^{-1}): 3291, 2366, 1605, 1250.

5-amino-3-(2-hydroxyphenyl)-1-phenyl-1H-pyrazole-4-carbonitrile (4b):
Yellow solid: ^{1}H NMR (400 MHz, $CDCl_3$) δ = 6.89 (t, 1H), 7.13 (d, 2H, ArH), 7.21-7.31 (m, 3H, ArH), 7.34 (t, 1H, ArH), 7.47 (d, 1H, ArH), 7.85 (d, 1H, ArH), 8.13 (s, 2H, NH_2), 10.83 (s, 1H, OH).

5-Amino-1-phenyl-3-(4-bromophenyl)-1*H*-pyrazole-4-carbonitrile (4d):
Light pink solid: ^{1}H NMR (400 MHz, $CDCl_3$) δ = 6.72 (t, 1H, ArH), 7.11 (d, 2H, ArH), 7.24 (t, 2H, ArH), 7.60 (q, 4H, ArH), 7.85 (s, 2H, NH_2); IR (KBr, cm^{-1}): 3302, 2371, 1592, 1254.

5-Amino-1-phenyl-3-(4-(trifluoromethyl)phenyl)-1*H*-pyrazole-4-carbonitrile (4l):
Cream colored solid: ^{1}H NMR (400 MHz, $CDCl_3$) δ = 6.81 (t, 1H, ArH), 7.11 (d, 2H, ArH), 7.23 (t, 2H, ArH), 7.67 (d, 2H, ArH), 7.80 (d, 2H, ArH), 7.91 (s, 2H, NH_2); IR (KBr, cm^{-1}): 3290, 2361, 1590, 1252.

General procedure for the synthesis of pyridines derivatives
A mixture of aromatic aldehydes (1 mmol), thiophenol (1 mmol) and malononitrile (2 mmol) were dissolved in water (5 mL) at room temperature, GO-TiO_2 (20 mg) was added as catalyst. Reaction mixture was continuously stirred for 1-2 h. The progress of the reaction was monitored by TLC. After completion, GO-TiO_2 catalyst removed by filtration. The GO-TiO_2 was further washed with ethanol (3x5 mL) and then dried under vacuum for reuse. Filtrate was treated with ethyl acetate (3x10 mL). The combined organic layers were treated with saturated brine solution and dried over anhydrous sodium sulphate. The removal of solvent yielded crude product, which was purified by chromatography over silica gel G-60 and afforded the desired products (79-89%).
The spectral data of selected synthesized pyridines derivatives are given below:

2-Amino-6-(cyclohexa-2,4-dienylthio)-4-phenylpyridine-3,5-dicarbonitrile (6a):
White solid: ^{1}H NMR (400 MHz, $CDCl_3$) δ = 7.00 (t, 1H, ArH), 7.13 (d, 2H, ArH), 7.22 (t, 2H, ArH), 7.23 (t, 1H, ArH), 7.39 (d, 2H, ArH), 7.48 (d, 2H, ArH), 7.80 (s, 2H, NH_2); IR (KBr, cm^{-1}): 3450, 3332, 2220, 1642, 1560.

2-Amino-4-(4-bromo-phenyl)-6-phenylsulfanyl-pyridine-3,5-dicarbonitrile (6b):
Yellow solid: ^{1}H NMR (400 MHz, $CDCl_3$) δ = 6.89 (t, 1H, ArH), 7.42(d, 2H, ArH), 7.55 (t, 2H, ArH), 7.60-7.65 (m, 2H, ArH) 7.79 (d, 2H, ArH), 7.89 (s, 2H, NH_2). IR (KBr, cm^{-1}): 3430, 3356, 2235, 1650, 1565.

Characterizations
The synthesised GO and GO-TiO_2 was characterized by Powder X-ray diffraction (PANalytical Empyrean). Morphology of the GO, and GO-TiO_2 were observed by Transmission Electron Microscope (TEM Hitachi H-7500), Field Emission-Scanning Electron Microscopy (FESEM, Supra 55 Carl Zeiss. Germany). The composition of the GO and GO-TiO_2 were determined by Energy-dispersive X-ray spectroscopy (EDAX) analysis on a (Electron Probe Microscope Oxford X-MAXn). FT-Raman spectra of GO and GO-TiO_2 was recorded on a (BRUKER RFS 27: Stand alone FT-Raman Spectrometer). Study the chemical state variations of the GO-TiO_2 composites, X-ray photoelectron (XPS) analysis on a PHI 5000 Versa Probe II, FEI Inc. Surface area of the GO and GO-TiO_2 were measured by a Brunauer–Emmett–Teller (BET) surface area analyzer (Quantumchrome Instrument 3200 Nova E). Electronic absorption spectral analysis was recorded on Shimadzu UV-1800 Spectrophotometer in the wavelength range of 200-800 nm. The FT-IR spectra were recorded on a (Perkin-Elmer RXI FT-IR Spectrometer) in KBr pellet. The ^{1}H NMR spectra of organic products were recorded in $CDCl_3$ on a (Bruker's advance III 400/500 MHz FT-NMR) at room temperature.

Results and discussion

The GO-TiO_2 composite was prepared by slight modification of the Patra et al.'s method.[20] The chemical and structural features of GO and GO-TiO_2 were elucidated by FT-IR, FT-Raman, PXRD, XPS FESEM, EDAX and TEM analyses.

FT-IR spectra of GO and GO-TiO_2

The chemical changes that occurred during the immobilization of TiO_2 nanoparticles onto GO were followed by FT-IR. The FT-IR spectra of GO, and GO-TiO_2 are shown in Fig 1. The FT-IR spectrum of GO (Fig. 1a) exhibited strong characteristics bands at 1035, 1223, 1623, 1731 and 3419 cm^{-1}, due to the presence of carboxylic, hydroxyl, phenolic, carbonyl, epoxy, etc. functional groups in the GO scaffold.[21] The FT-IR spectrum of GO-TiO_2, was found to be almost identical to the FT-IR spectrum of GO (Fig. 1b). However, additional sharp peaks observed in FT-IR spectrum of GO-TiO_2 at 564, 1002, 779 cm^{-1} which attributed to Ti-O-Ti, C-O-Ti vibrations.[22]

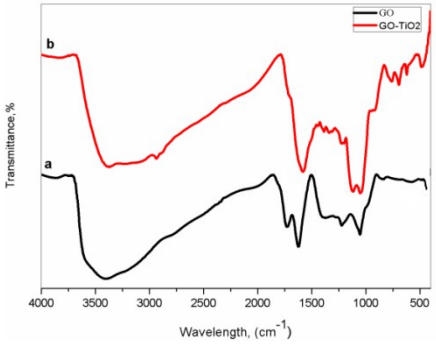

Figure 1. FTIR spectra of (a) GO and (b) GO-TiO_2.

FT-Raman spectra of GO and GO-TiO_2

The FT-Raman spectra of GO and GO-TiO_2 are shown in Fig. 2. The FT-Raman spectrum of GO and GO-TiO_2 show two remarkable peaks at around 1350, and 1593 cm^{-1} which were associated with the well-defined D band and G bands, respectively.[23] In additionally, new peaks are observed at about 149, 407, 517, 630 cm^{-1} which are assigned to the Eg, B1g, A1g, and Eg vibrations modes respectively in FT-Raman of GO-TiO_2 (Fig. 2b).[24] The values of ID/IG were found to be 0.83 and 0.88 for GO and GO-TiO_2 respectively. The increase in the ID/IG ratio is indicative of increasing disorder in the graphene oxide lattice after functionalization.[25]

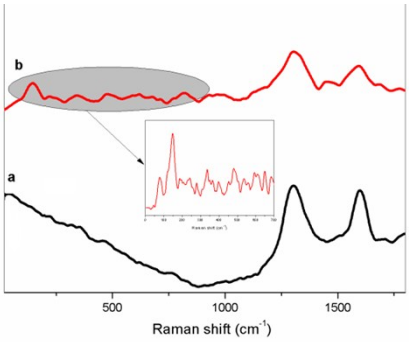

Figure 2. FT-Raman spectra of (a) GO and (b) GO-TiO_2.

Powder XRD spectra of GO and GO-TiO_2

The PXRD of GO and GO-TiO_2 are given in Fig. 3. The PXRD exfoliated GO (Fig. 3a) exhibited a broad diffraction peak at 2θ =

11.64° with a corresponding d spacing of 0.86 nm, which due to presence of functionalities in the basal plane of GO along with absorbed water molecules causing increase in the interlayer distance.[26] The PXRD spectrum of GO-TiO_2 (Fig. 3b) exhibited new peaks at 2θ = value of 25.62°, 37.98°, 48.14°, 54.12°, 55.34° were indexed to (101), (004), (200), (105) and (211) are readily indexed to the anatase phase of TiO_2.[27] The diffraction peak of GO disappeared in PXRD of GO-TiO_2, probably due to the disrupted layer-stacking regularity.[28]

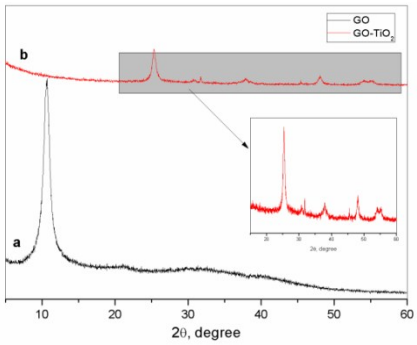

Figure 3. PXRD spectra of (a) GO and (b) GO-TiO_2.

X-ray photoelectron spectra of GO-TiO_2

In order to study the chemical state variations of the GO-TiO_2, X-ray photoelectron (XPS) analysis was utilized. Fig. 4a showing survey scan XPS spectrum demonstrates the presence of C, Ti and O species in GO-TiO_2 composites. Ti2p core level spectrum in Fig. 4b exhibits two bands located at binding energies 458.8 eV and 464.3 corresponding to Ti($2p^{3/2}$) and Ti($2p^{1/2}$) in the Ti^{4+} chemical state, respectively.[29] The deconvoluted O 1s XPS spectrum of the GO-TiO_2 has been shown in Fig. 4 c. The binding energy of 530.4 and 532.2 eV are attributed to the O-Ti and HO-Ti bonds respectively due to growth of TiO_2 on the graphene oxide surface. The diminished peaks centered at the binding energies of 531.4 and 533.6 eV are assigned to the C=O and C-OH functional groups, respectively.[30] This is consistent with the deconvoluted C 1s spectra (Fig. 4d) showing weaker residual oxygen containing functional group peaks compared to C=C , confirming the partial reduction of the GO during the composite formation.[31]

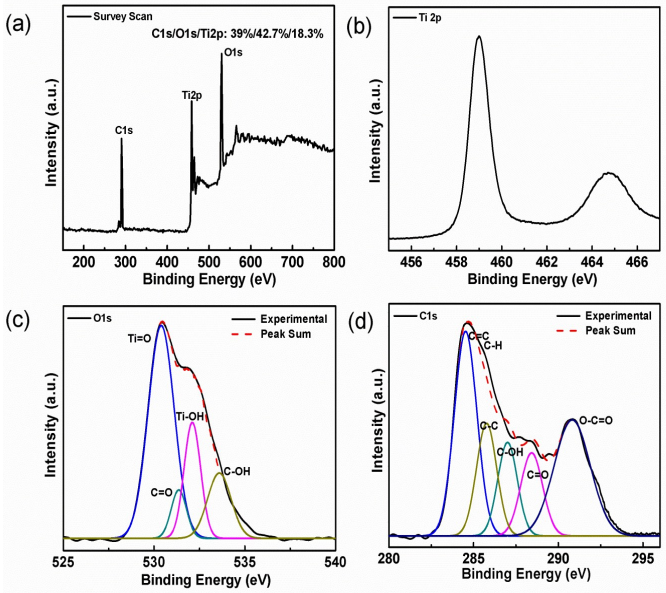

Figure 4. X-ray photoelectron survey spectra of (a) GO-TiO_2 (b) Ti 2p (c) deconvoluted O 1s and (d) deconvoluted C 1s XPS spectra of GO-TiO_2.

Micro-structural features and morphology analysis of GO and GO-TiO_2

Micro-structural features and morphology of GO and GO-TiO_2 were analyzed by FESEM (Fig. 5) and TEM (Fig. 6). The FESEM image of GO exhibited twisted nanosheets in disordered phase with a lot of wrinkles and crumpling features (Fig. 5a).[32] In Fig. 5b depicts the uniform distribution of TiO_2 nanoparticles on the graphene oxide sheets in FESEM image of GO-TiO_2. The TEM images of GO (Fig. 6a) revealed the nanoscopic features with few numbers of layers. The Fig. 6b also depicted the fine nanostructures of the GO-TiO_2, with homogeneous distribution of TiO_2 nanoparticles on the surface of GO. The EDAX analysis provides detailed chemical compositions on the GO and GO-TiO_2 (Fig. 7). The GO was found to be mainly composed of carbon and oxygen (Fig. 7a). The loading of TiO_2 nanoparticles on GO, changed the elemental composition with the introduction of titanium, apart from carbon and oxygen (Fig. 7b). Further, EDAX elemental mapping was performed to understand the distribution of the TiO_2 nanoparticles on GO surface (Fig. 8). The elemental mapping indicated the uniform distribution of Titanium over GO surface. The BET surface area of the GO and GO-TiO_2, determined by nitrogen physisorption at 77 K, was about 94.112 and 59.956 m^2g^{-1} respectively.

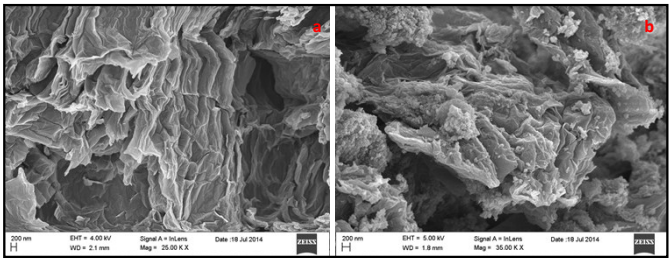

Figure 5. FEEM image of (a) GO and (b) GO-TiO_2.

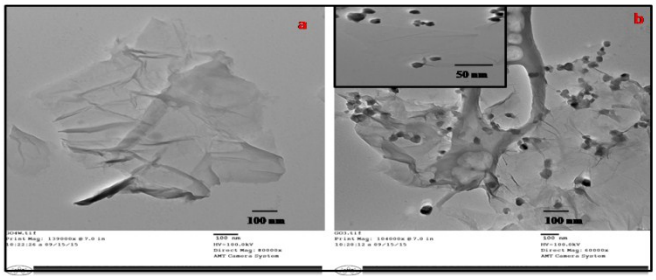

Figure 6. TEM image of (a) GO and (b) GO-TiO_2.

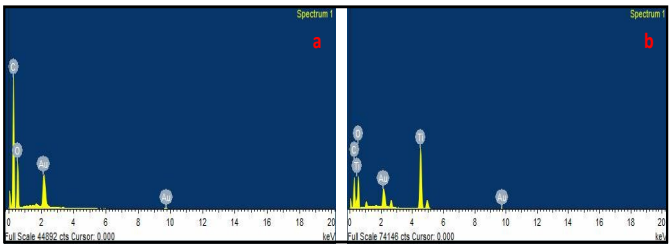

Figure 7. EDAX of (a) GO and (b) GO-TiO_2.

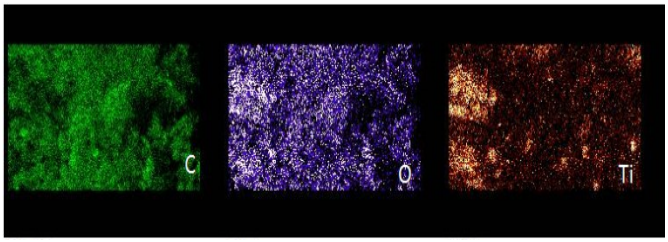

Figure 8. Elemental mapping images of carbon, oxygen and titanium in GO-TiO_2.

Catalytic application of GO-TiO_2

The catalytic efficiency of GO-TiO_2 was explored in the three component reactions of aldehydes, malonitrile and phenyl hydrazine shown in Scheme 1 and the three-component reactions of reaction of aldehydes, malononitrile and thiophenol shown in Scheme 2.

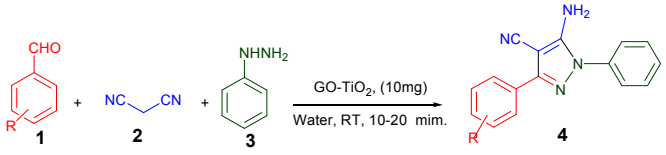

Scheme 1. Synthesis of pyrazoles derivatives using GO-TiO_2 as catalyst.

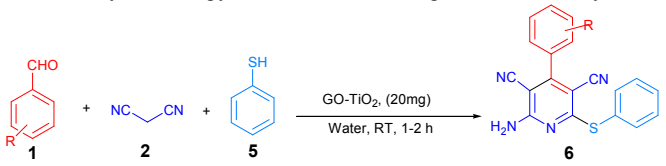

Scheme 2. Synthesis of pyridines derivatives using GO-TiO_2 as catalyst.

In order to optimize reaction conditions, various parameters such as, time, solvents and catalyst were studied. Benzaldehyde, malononitrile and phenyl hydrazine were chosen as model reactants for the synthesis of pyrazole derivatives at room temperature. These results are summarized in Table 1 When the reaction was carried out in absence of catalyst (Table 1, entry 1), no product was formed even after 08 h at room temperature. The same reaction in presence of 10 mg of GO in water (5 mL) at room temperature for 06 h yielded 30% of product (Table 1, entry 2). When the same reaction was carried out in the presence of TiO_2 (10 mg) in water for 06 h, 35% of product was yielded (Table 1, entry 3). However, when the reaction was carried out in the presence of GO-TiO_2 (10 mg) under room temperature in water, the desired product was obtained in 96% yield within 12 minutes (Table 1, entry 4). However, no significant improvement in the yield of the product was noticed when the catalyst loading was increased from 10 to 20 mg (Table 1, entry 5). It indicated that 10 mg of the catalyst was optimum. Among the various solvents used such as, water, ethanol, dichloromethane, acetonitrile, neat and dimethyl sulfoxide, water was found to be the best medium for the synthesis of pyrazole (Table 1, entries 1-10). The scope of the reaction was further extended to different aromatic aldehydes with malononitrile and phenyl hydrazine under the optimized reaction conditions and the products obtained, are summarized in Table 2. The electronic effect introduced by the substitution of the aromatic aldehyde had insignificant influence on the yields of the corresponding pyrazole derivatives. The products were obtained as white to dark yellow solid and characterized by FT-IR and ^{1}H NMR. All ^{1}H NMR of the products exhibited aromatic resonances between δ 6.71 to 7.89 and -N*H*$_2$ resonance between δ 7.85 to 8.33. The products, 5-amino-3-(2-hydroxyphenyl)-1-phenyl-1H-pyrazole-4-carbonitrile(**4b**) and 5-amino-3-(5-bromo-2-hydroxyphenyl)-1-phenyl-1H-pyrazole-4-carbonitrile **(4h)** showed a broad peak at δ 11.01 and 11.36 respectively, due to -O*H* group attached to the aromatic ring. The proton of the -C*H*O group attached to aromatic ring was observed as sharp singlet at δ 10.05 in *5-amino-3-(4-formylphenyl)-1-phenyl-1H-pyrazole-4-carbonitrile* **(4e).**All data matches well with the literature values.[16]

Table 1. Optimization of Reaction Conditions for the synthesis of pyrazole derivatives from benzaldehyde, malonitrile and phenyl hydrazine at room temperature[a]

Entry	Catalyst (mg)	Time (h)	Solvents	Yield, %[b]
1	---	08	Water	--
2	GO (10)	06	Water	30
3	TiO_2 (10)	06	Water	35
4	GO-TiO_2 (10)	0.2	Water	96
5	GO-TiO_2 (20)	0.2	Water	96
6	GO-TiO_2 (10)	0.2	Ethanol	84
7	GO-TiO_2 (10)	0.2	DCM	81
8	GO-TiO_2 (10)	0.2	Acetonitrile	90
9	GO-TiO_2 (10)	0.2	--	72
10	GO-TiO_2 (10)	0.2	DMSO	76

[a]Reaction conditions: benzaldehyde (1mmol), malonitrile (1mmol), phenyl hydrazine (1 mmol).
[b] Isolated yield after work up.

Table 2. Synthesis of pyrazoles derivatives from aldehydes, malonitrile and phenyl hydrazine catalyzed by GO-TiO_2

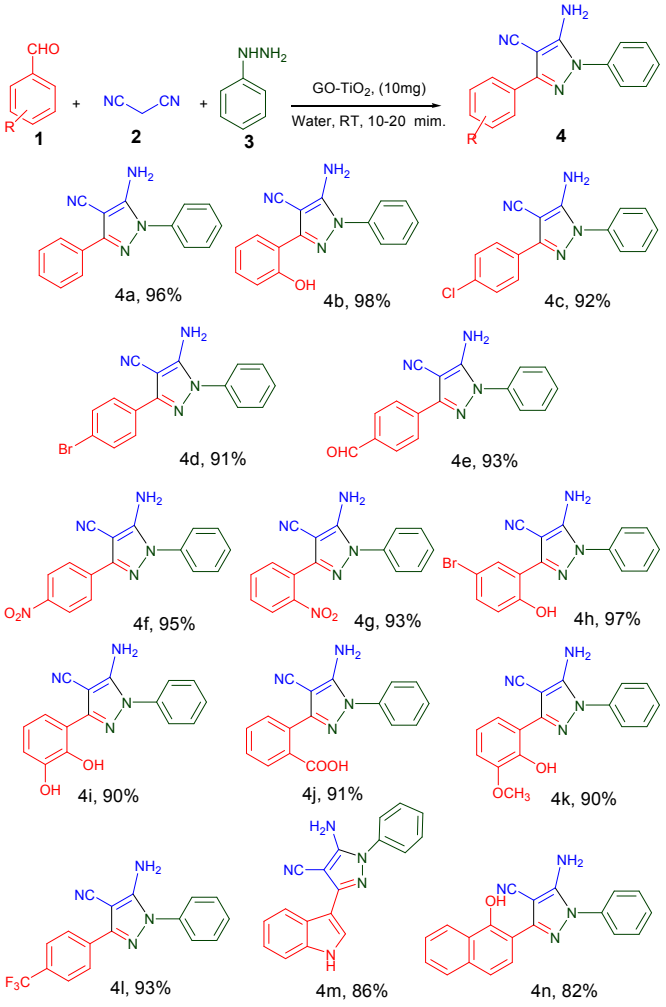

In order to find out the optimum reaction conditions for the synthesis of pyridines derivatives benzaldehyde, malonitrile and thiophenol were chosen as model reactants (Table 3). When the reaction was carried out without catalyst (Table 3, entry 1), no product was formed after 24 h. When (10 mg) GO as a catalyst (Table 3, entry 2) in water for 24 h at room temperature, no product was obtained; only starting material was obtained as such. TiO_2 nanoparticles alone (10 mg) under identical conditions, afforded product in 15% yield (Table 3, entry 3). However, when reaction was carried out with 10 mg GO-TiO_2 in water, at room temperature the desired product was obtained in 72% yield within 2 h (Table 3, entry 4) However, significant improvement in yield of the product was noticed when the catalyst loading was increased from 10 to 20 mg (Table 3, entry 5). Further increase in amount of catalyst has no

effect on the yield of the desired product (Table 3, entry 6). Among the various solvents used such as DCM, acetonitrile, neat and DMSO, water was found to be the best solvent for the reactions (Table 3, entries 1–10). After optimization of the reaction conditions, we choose a variety of different aldehydes with malononitrile and thiophenol to discern the catalytic scope and the generality of the GO-TiO_2 (Table 4). Aryl aldehydes, possessing electron withdrawing groups, afforded better results as compared to aldehydes bearing electron donating groups. The products were obtained as white to brownish solid and fully characterized by FT-IR and ^{1}H NMR. All ^{1}H NMR of the products exhibited aromatic resonances between δ 6.89 to 7.90 and -NH_2 resonance between δ 7.80 to 7.98. The products, 2-amino-4-(2-hydroxyphenyl)-6-(phenylthio)pyridine-3,5-dicarbonitrile **(6c),** 2-amino-4-(4-methoxyphenyl)-6-(phenylthio)pyridine-3,5-dicarbonitrile **(6d),** and 2-amino-4-(4-formylphenyl)-6-(phenylthio)pyridine-3,5-dicarbonitrile **(6e)** showed a peak at δ 11.01, 3.35 and 10.09 due to -O*H*, -CH_3 and -C*H*O group attached to aromatic ring, respectively. These NMR data were in consonance with the earlier reports[17] and confirms the formation of the desired product.

Table 3. Optimization of Reaction Conditions for the synthesis of pyridine derivatives from benzaldehyde, malonitrile and thiophenol at room temperature[a]

Entry	Catalyst (mg)	Time(h)	Solvents	Yield, %[b]
1	---	24	Water	--
2	GO (10)	24	Water	--
3	TiO_2 (10)	24	Water	15
4	GO-TiO_2 (10)	02	Water	72
5	GO-TiO_2 (20)	02	Water	85
6	GO-TiO_2 (30)	02	Water	85
7	GO-TiO_2 (20)	02	DCM	80
8	GO-TiO_2 (20)	02	Acetonitrile	79
9	GO-TiO_2 (20)	02	--	65
10	GO-TiO_2 (20)	02	DMSO	71

[a]Reaction conditions: benzaldehyde (1mmol), malonitrile (2mmol), thiophenol (1 mmol).
[b] Isolated yield after work up.

Table 4. Synthesis of pyridines derivatives from aldehydes, malonitrile and thiophenol catalyzed by GO-TiO_2

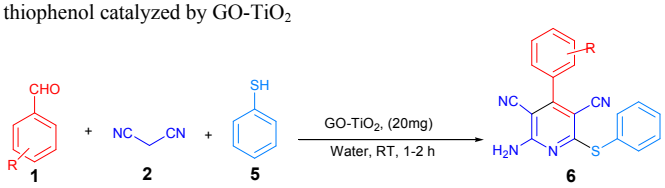

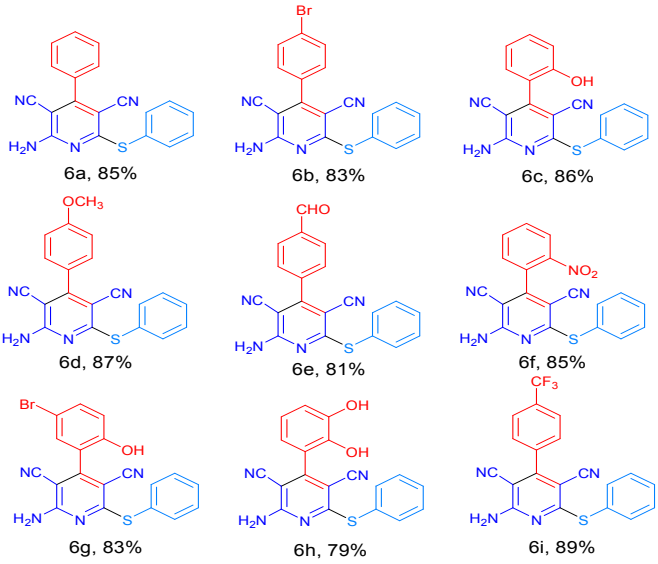

Mechanistic considerations

The mechanistic aspect of the reaction is ambiguous at present, however, a plausible mechanism involving an $\dot{O}_2$ radical has been proposed (Scheme 3). We speculate that the unpaired electrons present at the edge of GO[32-34] react with the atmospheric oxygen to generate, which subsequently reacts with malononitrile to generate radical (I_1). Condensation of an aldehyde with I_1 leads to the corresponding Knoevenagel product I_2. The thiophenol is deprotonated by the $\dot{O}_2$ to form thiolate anion (I_3). Next, the second molecule of malononitrile undergoes Michael addition followed by simultaneous thiolate addition to CN^- which undergoes oxidative aromatization to provide pyridine derivatives.[12b]

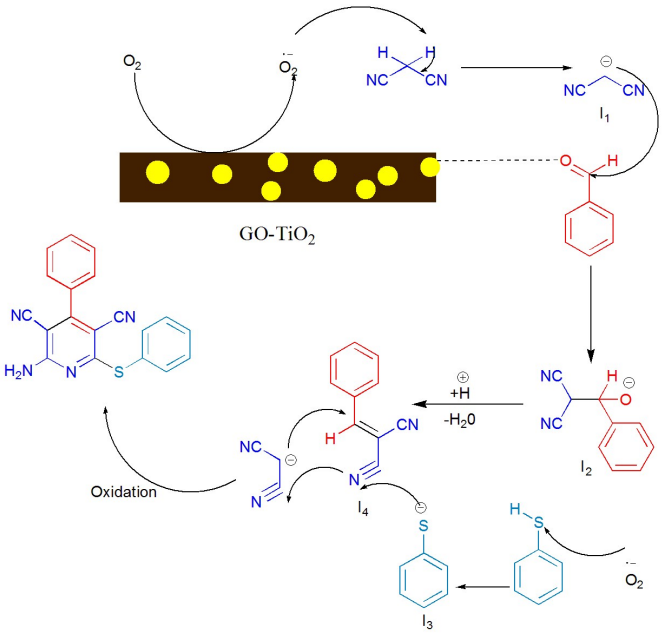

Scheme 3. Proposed reaction mechanism for the formation of pyridines derivatives.

Recyclability test

Furthermore, the catalyst was tested for recyclability up to seven times for the synthesis of pyrazole from benzaldehyde, malononitrile, and phenyl hydrazine. It is apparent from (Fig. 9) that the GO-TiO_2 catalyst could be reused up to five cycles without loss

of catalytic activity. However, gradual decline in the catalytic activity of GO-TiO_2 was noted after 6th cycle.

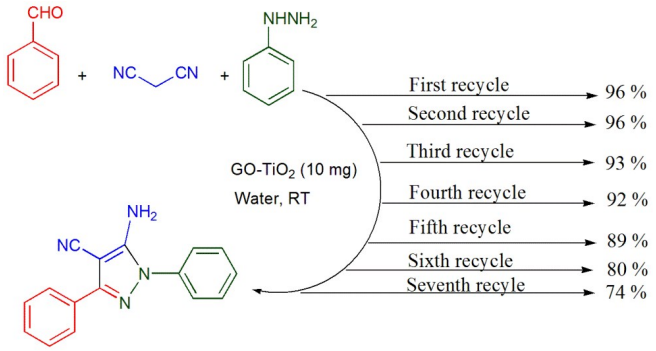

Figure 9. Recyclability of the catalyst

Conclusions

In summary, Graphene oxide-TiO_2 composites (GO-TiO_2) has been synthesised and fully characterized by FT-IR, FT-Raman, XRD, XPS, FESEM, TEM, EDAX, and N_2 adsorption–desorption. The GO-TiO_2 has been found to be an efficient heterogeneous catalyst for the synthesis pyrazoles derivatives from aldehydes, malononitrile, and phenyl hydrazine and pyridines derivatives from aldehydes, thiophenol and malononitrile in aqueous medium at room temperature in high yields. The developed catalyst is very cheap, easily recovered at the end of the reaction, and recycled up to five times without significant loss in catalytic activity.

Notes and references

[a] Department of Applied Chemistry, Indian School of Mines, Dhanbad-826004, India

[b] Department of Chemistry, Vidya Vihar Institute of Technology, Purnea-854303, India

Email: Shweta@ac.ism.ac.in (Shweta Kumari), amiyashekhar@gmail.com (Amiya Shekhar), ddpathak61@gmail.com (DD Pathak)*

*Phone number: +91 9431126250

We are thankful to the CRF ISM, SAIF IIT Madras, SAIF Panjab University, STIC, Kochi, and IISER Bhopal for providing help in the analysis of the samples. SK acknowledges the receipt of ISM fellowship.

1 (*a*) X. Yang, Y. Tu, L. Li, S. Shang and X. M. Tao, *ACS Appl. Mater. Interfaces*, 2010, **2**, 1707-1713; (*b*) Y. Matsumoto, M. Koinuma, S. Ida, S. Hayami, T. Taniguchi, K. Hatakeyama, H. Tateishi, Y. Watanabe and S. Amano, *J. Phys. Chem. C*, 2011, **115**, 19280-19286; (*c*) Y. Zhu, D. K. James and J. M. Tour, *Adv. Mater.*, 2012, **24**, 4924-4955; (*d*) S. H. Lee, H. W. Kim, J. O. Hwang, W. J. Lee, J. Kwon, C. W. Bielawski, R. S. Ruoff and S. O. Kim, *Angew. Chem. Int. Ed.*, 2010, **49**, 10084-1088.

2 (*a*) S. S. Li, J. J. Lv, Y. Y. Hu, J. N. Zheng, J. R. Chen, A. J. Wang and J. J. Feng, *J. Power Sources*, 2014, **247**, 213-218; (*b*) Y. L. Min, K. Zhang, W. Zhao, F. C. Zheng, Y. C. Chen and Y. G. Zhang, *Chem. Eng. J.*, 2012, **194**, 203-210; (*c*) H. P. Mungse, S. Verma, N. Kumar, B. Sain and O. P. Khatri, *J. Mater. Chem.*, 2012, **22**, 5427-5433; (*d*) Z. Li, S. Wu, H. Ding, Da. Zheng, J. Hu, X. Wang, Q. Huo, J. Guan and Q. Kan, *New J. Chem.*, 2013, **37**, 1561-1568; (*e*) P. K. Khatri, S. Choudhary, R. Singh, S. L. Jain and O. P. Khatri, *Dalton Trans.*, 2014, **43**, 8054-8061; (*f*) H. Su, Z. Li, Q. Huo, J. Guan and Q. Kan, *RSC Adv.*, 2014, **4**, 9990-9996.

3 (*a*) Q. Li, B. Guo, J. Yu, J. Ran, B. Zhang, H. Yan and J. R. Gong, *J. Am. Chem. Soc.*, 2011, **133**, 10878-10884; (*b*) Y. Liang, H. Wang, H. S. Casalongue, Z. Chen and H. Dai, *Nano Res.*, 2010, **3**, 701-705; (*c*) T. Jiang, Z. Tao, M. Ji, Q. Zhao, X. Fu and H. Yin, *Catal. Commun.*, 2012, **28**, 47-51.

4 (*a*) Y. Zhang, Z. R. Tang, X. Fu and Y. J. Xu, *ACS Nano*, 2010, **4**, 7303-7311; (*b*) Y. Zhang, Z. R. Tang, X. Fu, and Y. J. Xu, *ACS Nano*, 2011, **5**, 7426-7435; (*c*) N. Zhang, Y. Zhang and Y. J. Xu, *Nanoscale*, 2012, **4**, 5792-5813; (*d*) M. Q. Yang, N. Zhang, M. Pagliaro and Y. J. Xu, *Chem.Soc.Rev.*, 2014, **43**, 8240-8254; (*e*) N. Zhang, M. Q. Yang, S. Liu, Y. Sun, and Y. J. Xu, *Chem.Rev.*, 2015, **115**, 10307-10377; (*f*) N. Zhang and Y. J. Xu, *CrystEngComm*, 2016, **18**, 24-37.

5 (*a*) S. Kumari, A. Shekhar and D. D. Pathak, *RSC Adv.*, 2014, **4**, 61187-61192; (*b*) S. Kumari, A. Shekhar, H. P. Mungse, O. P. Khatri and D. D. Pathak, *RSC Adv.*, 2014, **4**, 41690-41695; (*c*) L. Yuan, Q. Yu, Y. Zhang and Y. J. Xu, *RSC Adv.*, 2014, **4**, 15264-15270 (*d*) S. Kumari, A. Shekhar and D. D. Pathak, *RSC Adv.*, 2016, **6**, 15340-15344; (*e*) X. Li, B. Weng, N. Zhang and Y. J. Xu, *RSC Adv.*, 2014, **4**, 64484-64493.

6 (*a*) A. Dhakshinamoorthy, S. Navalon, A. Corma and H. Garcia, *Energy Environ. Sci.*, 2012, **5**, 9217-9233; (*b*) X. Chen, L. Liu, P. Y. Yu and S. S. Mao, *Science*, 2011, **331**, 746-750; (*c*) S. K. Choi, S. Kim, S. K. Lim and H. Park, *J. Phys. Chem. C*, 2010, **114**, 16475-16480; (*d*) A. L. Linsebigler, G. Lu and J. T. Yates, *Chem. Rev.*, 1995, **95**, 735-758; (*e*) X. Chen and S. S. Mao, *Chem. Rev.*, 2007, **107**, 2891-3361.

7 Z. Liu, X. Zhang, S. Nishimoto, T. Murakami and A. Fujishima, *Environ. Sci. Technol.*, 2008, **42**, 8547–8551.

8 L.W. Zhang, H.-Bo Fu and Y.F. Zhu, *Adv.Funct. Mater.*, 2008, **18**, 2180-2189.

9 J. H. Byeon and J. W. Kim, *J. Mater. Chem. A.*, 2014, **2**, 6939-6944.

10 D. S. R. Josephine, B. Sakthivel, K. Sethuraman, and A. Dhakshinamoorthy, *ChemPlusChem*, 2015, **80**, 1472–1477.

11 J. Khalafy, A. P. Marjani, F. Salami, *Tetrahedron Lett.*, 2014, **55** 6671-6674.

12 (*a*) F. Nemati, S. H. Nikkhah, A. Elhampour, *Chinese Chemical Letters*, 2015, **26**, 1397–1399; (*b*) P. Manna, P. K. Maiti, *Tetrahedron Lett.*, 2015, **56**, 5094–5098.

13 (*a*) A.M. Mohamed, W.A. El-Sayed, M.A. Alsharari, *Arch. Pharm. Res.* 2013, **36** 1055–1065; (*b*) S.G. Alegaon, K.R. Alagawadi, M.K. Garg, K. Dushyant and D. Vinod, *Bioorg. Chem.* 2014, **54**, 51–59; (*c*) R. Sridhar, P.T. Perumal and S. Etti, *Bioorg. Med. Chem. Lett.*, 2004, **14**, 6035–6040.

14 (*a*) I. Celik, N. Kanıskan and S. Kokten, *Tetrahedron,* 2009, **65**, 328; (*b*) C. Kashima, Y. Miwa, S. Shibata and H. Nakozono, *J. Heterocycl. Chem.*, 2003, **40**, 681.

15 (a) V. Perrier, A. C. Wallace, K. Kaneko, J. Safar, S. B. Prusiner and F. E. Cohen, *Proc. Natl. Acad. Sci. U.S.A.* 2000, **97**, 6073; (b) A. A. Nirschl, L. G. Hamann, *US Pat. Appl. Publ.* 2005, **182**, 105.

16 S. Maddila, S. Rana, R. Pagadala, S. Kankala, S. Maddila, S. B. Jonnalagadda, *Catalysis Commun.*, 2015, **61**, 26–30.

17 (*a*) S. Mishra and R. Ghosh, *Synth. Commun.*, 2012, **42**, 2229-2244; (*b*) K. Guo, M. J. Thompson and B. J. Chen, *Org. Chem.*, 2009, **74**, 6999-7006.

18 M. Srivastava, P. Rai, J. Singh and J. Singh, *RSC Adv.*, 2013, **3**, 16994-16998.

19 N. I. Kovtyukhova, P. J. Ollivier, B. R. Martin, T. E. Mallouk, S. A. Chizhik, E. V. Buzaneva and A. D. Gorchinskiy, *Chem. Mater.*, 1999, **11**, 771–778.

20 A. K. Patra, S. K. Das and A. Bhaumik, *J. Mater. Chem.*, 2011, **21**, 3925-3930.

21 (*a*) T. Szabo, O. Berkesi and I. Dekany, *Carbon,*2005, ***43***, 3186-3189; (*b*) A. Bagri, C. Mattevi, M. Acik, Y. J. Chabal, M. Chhowalla and V. B. Shenoy, *Nat. Chem.*, 2010, ***2***, 581-587.

22 Y. Zhang, C. Zhong, Q. Zhang, B. Chen, M. He and B. Hu, *RSC Adv.*, 2015, **5**, 5996–6005.

23 (*a*) K. N. Kudin, B. Ozbas, H. C. Schniepp, R. K. Prud'homme, I. A. Aksay and R. Car, *Nano Lett.,* 2008, **8**, 36-41; (*b*) G. K. Ramesha and S. Sampath, *J. Phys. Chem. Lett.,* 2009, ***113,*** 7985-7989.

24 K. Dai, L. Lu, Q. Liu, G. Zhu, Q. Liua and Z. Liua, *Dalton Trans.*, 2014, **43**, 2202-2210.

25 M. Ali Nasseri, A. Allahresani and H. Raissi, *RSC Adv.*, 2014, **4**, 26087-26093.

26 F. Liu, J. Sun, L. Zhu, X. Meng, C. Qi and F.-S. Xiao, J. Mater. Chem., 2012, **22**, 5495-5502.

27 J. H. Byeon and J.W. Kim *J. Mater. Chem. A.*, 2014, **2**, 6939-6944.

28 Liu, H. Bai, Y. Wang, Z. Liu, X. Zhang and D. D. Sun, *Adv. Funct. Mater.*, 2010, **20**, 4175-4181.

29 O. Akhavan and E. Ghaderi, *J. Phys. Chem. C*, 2009, **113**, 20214-20220.

30 D. Zhao, G. Sheng, C. Chen and X. Wang, *Appl Catal B: Environ*., 2012, **111**, 303-308.

31 S. K. Ujjain, P. Ahuja and R. K. Sharma, *J. Mater. Chem. A,* 2015, **3**, 9925-9931.

32 (*a*) C. K. P. Neeli, S. Ganji, V. S. P. Ganjala, S. R. R. Kamarajua and D. R. Burri, *RSC Adv*., 2014, **4**, 14128–14135; (*b*) N. Anand, K. H. P. Reddy, K. S. R. Rao and D. R. Burri, *Catal. Lett*., 2011, **141**, 1355–1363.

33 (*a*) C. Su, M. Acik, K. Takai, J. Lu, S. Hao, Y. Zheng, P. Wu, Q. Bao, T. Enoki, Y. J. Chabal and K. P. Loh, *Nature Commun.*, 2012, **3**, 1298-1306; (*b*) V. Stengl, J. Henych, P. Vomacka and M. Slusn *Photochem. Photobiol.,* 2013, **89**, 1038-1046

34 (*a*) M. Wang, X. Song and N. Ma, *Catal. Lett*., 2014, **144**, 1233-1239; (*b*) L. S. Bai, X. M. Gao, X. Zang, F. F. Sun and N. Ma, *Tetrahedron Lett.,*2014, **55**, 4545-4548.

Graphical Abstract

The GO-TiO_2 has been found to be highly efficient and recyclable heterogeneous catalyst for the synthesis of pyrazoles and pyridines in aqueous medium at room temperature.